

# Crystallization and preliminary X-ray crystallographic studies of recombinant human betaine–homocysteine S-methyltransferase

Nandita Bose and Cory Momany\*

Department of Pharmaceutical and Biomedical Sciences, Wilson College of Pharmacy, University of Georgia, Athens, GA 30602, USA

Correspondence e-mail: cmomany@rx.uga.edu

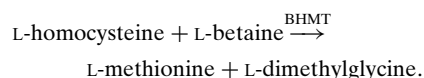
Betaine–homocysteine S-methyltransferase (BHMT) catalyzes a reaction essential for regulation of methionine and homocysteine metabolism and the catabolism of choline in mammalian tissues. Human recombinant BHMT (MW = 45 kDa) has been crystallized by the hanging-drop vapor-diffusion method at 294 K using ethylene glycol as the precipitant. The crystals belong to the monoclinic space group C2, with unit-cell parameters  $a = 109.190$ ,  $b = 91.319$ ,  $c = 88.661$  Å,  $\beta = 122.044^\circ$ , and diffract to 2.9 Å resolution on a local rotating-anode X-ray source. Rotation-function analysis and the Matthews coefficient,  $V_M = 2.46$  Å<sup>3</sup> Da<sup>-1</sup>, are consistent with a dimer in the asymmetric unit, suggesting that the active enzyme is a tetramer with 222 symmetry.

Received 5 October 2000

Accepted 19 December 2000

## 1. Introduction

Regulation of homocysteine metabolism has gained recent attention since epidemiological studies established that homocysteine is an independent risk factor, even with only moderate elevations in the plasma, for the development of arteriosclerotic vascular disease (Finkelstein & Martin, 1984*b*). The enzyme betaine–homocysteine S-methyltransferase (BHMT; E.C. 2.1.1.5) has an important role in the modulation of plasma homocysteine in that it catalyzes the reaction



The only other enzyme known to methylate homocysteine in mammalian cells is the folate/vitamin B<sub>12</sub> dependent methionine synthase (E.C. 2.1.1.13). The reaction catalyzed by BHMT is significant in the regulation of methionine metabolism both as a means for the maintenance of hepatic concentrations of methionine during periods of inadequate intake of this amino acid (Finkelstein *et al.*, 1982) and for the removal of excessive homocysteine (Finkelstein *et al.*, 1978). In addition to the key role of BHMT in methionine metabolism, the utilization of betaine by BHMT is an obligatory reaction in the catabolism of choline in mammalian tissues.

*In vitro* studies indicate that homocysteine remethylation is shared equally between BHMT and methionine synthase. Large oral doses of betaine have been used therapeutically to reduce homocysteine (Mudd *et al.*, 1995) in patients suffering from homocystinuria. The efficacy of betaine treatment is a consequence, at least in part, of increased

methylation of homocysteine by the BHMT-catalyzed reaction. BHMT is therefore a pharmacologically interesting target for the treatment of homocystinuria, since a better methyl donor than betaine may have more potent plasma homocysteine lowering effects.

BHMT is a zinc metalloenzyme (Millian & Garrow, 1998) that shares limited similarity to the amino-terminal region of bacterial and eukaryotic methionine synthases (Garrow, 1996). Previous studies on the liver enzyme isolated from rats have shown that it is inhibited by S-adenosylmethionine (SAM; Finkelstein & Martin, 1984*a*). However, BHMT does not appear to contain a SAM-binding motif recognizable by sequence analysis. All these biochemical aspects of the enzyme could be better understood if the atomic structure of the enzyme were known. Structural information obtained by X-ray crystallographic studies could be helpful in identifying the critical residues involved in its mechanism and could also predict mutations in BHMT that could make individuals predisposed to heart disease. Further, drugs that act as more efficient methyl donors could be useful therapeutically. Here, we report the crystallization and preliminary diffraction analysis of human recombinant BHMT.

## 2. Materials and methods

### 2.1. Cloning, expression and purification of BHMT

The DNA encoding BHMT was amplified by PCR from a human cDNA library (Stratagene) and cloned into an expression vector, a modified pET28b, to contain a polyhistidine purification tag at the N-terminus of the protein.

Details concerning the construction of the expression plasmid will be reported in detail elsewhere. Expression was performed at room temperature using BL21 Codon Plus (DE3) cells (Stratagene) in LB media supplemented with 250  $\mu$ M zinc chloride. Cells were sonicated in 0.5 M NaCl, 20 mM potassium phosphate pH 7.4, centrifuged at 60 000g and the clarified supernatant purified by Ni<sup>2+</sup> metal-chelate affinity chromatography with a Pharmacia NTA Hi-Trap column using an imidazole gradient for elution (0–0.5 M imidazole, 0.5 M NaCl, 20 mM potassium phosphate pH 7.4). After purification, the protein was dialyzed into 50 mM Tris–HCl buffer pH 8.0. A second purification step using a Pharmacia Hi-Trap Q column was introduced (elution: 0–1.0 M NaCl, 50 mM Tris–HCl pH 8.0) to improve crystal diffraction quality.

## 2.2. Crystallization

A broad range of crystallization conditions following the sparse-matrix sampling method (Jancarik & Kim, 1991) were examined by vapor-diffusion (McPherson, 1976) trials using 2  $\mu$ l drops of protein incubated with equal volumes of well solutions from Crystal Screens 1 and 2 and PEG,

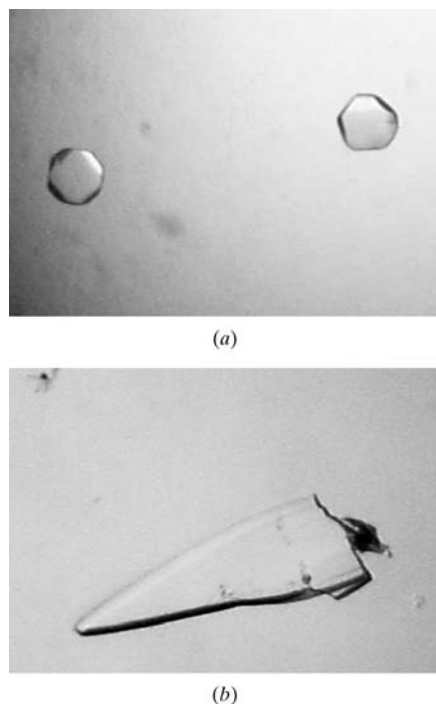


**Figure 1**  
(a) Crystals of human BHMT obtained using PEG 20 000 and ethylene glycol (protein concentration, 7 mg ml<sup>-1</sup>). (b) Crystal of different morphology obtained using a lower protein concentration (4 mg ml<sup>-1</sup>) but otherwise identical conditions.

and PEG/lithium chloride kits from Hampton Research.

## 2.3. Data collection and processing

Immediately prior to data collection, a single plate-like crystal was quickly transferred into a cryoprotectant solution containing 30% (v/v) 2,3-butanediol and 70% (v/v) artificial mother liquor (13% PEG 20000, 8% ethylene glycol, 0.1 M HEPES pH 7.5). The crystal was flash-cooled to 100 K in a nitrogen stream produced by an MSC X-STREAM cooling system. X-ray data were collected using a Rigaku R-AXIS IIC image-plate detector mounted on a Rigaku RU-200 rotating-anode X-ray (Cu K $\alpha$ ) generator equipped with Osmic mirrors and operating at 50 kV and 100 mA. The data was processed using the DENZO and SCALEPACK programs from the HKL2000 suite (Otwinowski & Minor, 1997).

## 3. Results and discussion

Initial crystallization conditions were obtained with 10 mg ml<sup>-1</sup> protein and 5% PEG 6000 as precipitant with protein purified in the single metal-chelate column step. Tiny crystals appeared the day following setup, but they did not increase in size after the initial growth. Unsuccessful optimization

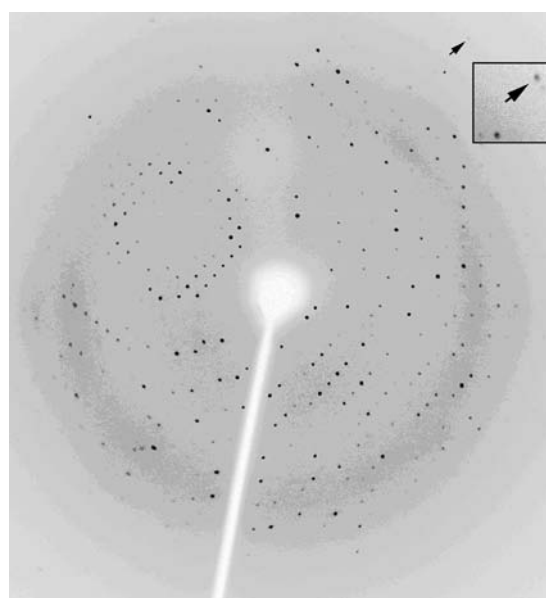


**Figure 2**  
A typical diffraction pattern of a crystal of recombinant human BHMT. Shown is an image as represented by the HKL2000 data-processing package. Data-collection settings were: crystal-to-detector distance, 200 mm; oscillation range, 1.0°; exposure time, 10 min; total frames collected, 180. The arrow at the top right of the figure points to a reflection at 2.9 Å resolution. The inset is a magnified window around the arrow.

**Table 1**  
Data-collection statistics.

Values in parentheses are for the outer resolution shell.	
Wavelength (Å)	1.5418
Space group	C2
Unit-cell parameters	
<i>a</i> (Å)	109.190
<i>b</i> (Å)	91.319
<i>c</i> (Å)	88.661
$\beta$ (°)	122.044
<i>V</i> (Å <sup>3</sup> )	884041
No. of observed reflections	51853
No. of unique reflections	14797
Resolution range (Å)	30.0–3.0 (3.05–3.0)
Completeness (%)	94.2 (70.1)
<i>I</i> / $\sigma$ ( <i>I</i> ) > 3 (%)	75.3 (60.0)
<i>R</i> <sub>merge</sub> † (%)	8.5 (36.1)

$$\dagger R_{\text{merge}} = \frac{\sum_h \sum_i |I(h)_i - \langle I(h) \rangle|}{\sum_h \sum_i I(h)_i}$$

trials included the addition of additives such as salts (sodium chloride, lithium chloride, ammonium chloride and ammonium sulfate) and organics (dioxane and glycerol). Since optimization of the initial conditions failed to produce large crystals, an additional purification step, ion-exchange chromatography using a Pharmacia Hi-Trap Q column, was introduced. Crystal Screens 1 and 2 were again screened with the higher quality protein. Crystals with a hexagonal morphology, which unfortunately failed to diffract, were obtained from 10 mg ml<sup>-1</sup> protein in 20 mM Tris–HCl pH 8.0 with well

solutions containing 10% (w/v) PEG 8000, 8% (w/v) ethylene glycol, 0.1 M Na HEPES pH 7.5. Ethylene glycol at 8% (w/v) was absolutely essential for crystal formation. Additional optimization included screening with PEGs 400, 600, 2000, 3000, 5000 and 20 000. Two different types of crystals were obtained from similar conditions. Condition 1 (Fig. 1a) consisted of 2  $\mu$ l of 7 mg ml<sup>-1</sup> protein, 3% PEG 20 000 and 3% ethylene glycol crystallized with 2  $\mu$ l of the well solution containing only 8% ethylene glycol. These crystals appeared in a week. Condition 2 (Fig. 1b) consisted of 2  $\mu$ l of 4 mg ml<sup>-1</sup> protein with the same conditions as condition 1. These clear plate-like crystals appeared in four weeks. Crystals obtained from condition 1 failed to diffract, while the crystals obtained by condition 2 diffracted to 2.9 Å resolution.

The diffraction data collected on an area detector (Fig. 2) were

consistent with the space group  $C2$ . Diffraction spots were observable at  $2.9 \text{ \AA}$  resolution, but the data set was processed to  $3.0 \text{ \AA}$  with an overall  $R_{\text{merge}}$  of 8.5%. Diffraction is anisotropic, which is consistent with a plate-like crystal. The refined unit-cell parameters were  $a = 109.190$ ,  $b = 91.319$ ,  $c = 88.661 \text{ \AA}$ ,  $\beta = 122.044^\circ$ . Data-collection statistics are summarized in Table 1. The molecular weight of the monomer is 45 kDa; therefore, assuming two molecules per asymmetric unit, the Matthews coefficient  $V_M$  is  $2.46 \text{ \AA}^3 \text{ Da}^{-1}$ , corresponding to a solvent-volume fraction of 49.5%

(Matthews, 1968). The unit-cell volume is  $884\,041 \text{ \AA}^3$ .

Using the area-detector data, self-rotation functions were calculated using the program *GLRF* (Tong & Rossmann, 1997) to identify likely non-crystallographic symmetry. The rotation-function analyses, calculated with  $30.0\text{--}4.0 \text{ \AA}$  resolution data and a radius of integration of  $20 \text{ \AA}$ , showed only strong peaks at  $\kappa = 180^\circ$  (Fig. 3) that would be consistent with non-crystallographic twofold axes perpendicular to the crystallographic  $b$  axis ( $\psi = 90^\circ$ ,  $\varphi = 55^\circ$ ) rotated  $55^\circ$  from the  $a$  axis. The non-crystallographic twofold symmetry and the crystallographic  $C2$  symmetry support the likelihood that the protein is a tetramer with molecular 222 symmetry, but this is inconsistent with earlier assumptions that BHMT is a hexamer (Lee *et al.*, 1992). This discrepancy requires closer scrutiny, since our recombinant protein contains a polyhistidine tag at the N-terminus that could interfere with proper oligomerization, but the prediction that the protein is a hexamer is based on studies on the rat liver enzyme and may not hold in the case of the human enzyme.

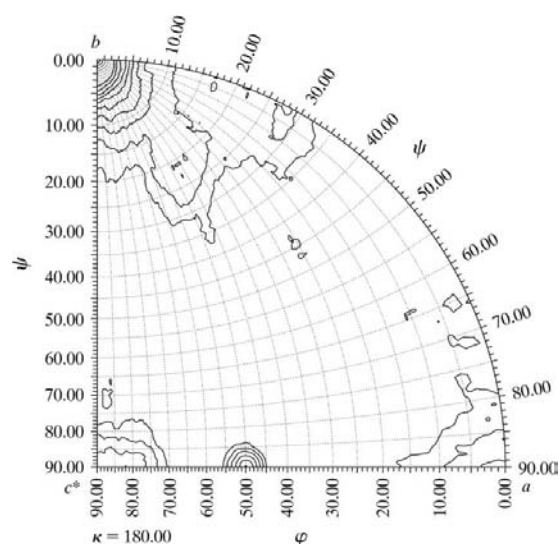


**Figure 3**  
Self-rotation function of a BHMT crystal calculated using *GLRF* (Tong & Rossmann, 1997).

The authors wish to thank James Liu, John Rose and Bi-Cheng Wang of the Department

of Biochemistry, UGA for providing beam time on the R-AXIS area detector and for assistance in data collection, and Tammy Dailey for a sample of the cDNA used for construction of the expression vector. This research was supported by a grant to CM from the University of Georgia Research Foundation.

## References

- Finkelstein, J. D. & Martin, J. J. (1984a). *Biochem. Biophys. Res. Commun.* **118**, 14–19.
- Finkelstein, J. D. & Martin, J. J. (1984b). *J. Biol. Chem.* **259**, 9508–9513.
- Finkelstein, J. D., Martin, J. J., Harris, B. J. & Kyle, W. E. (1982). *Arch. Biochem. Biophys.* **218**, 169–173.
- Finkelstein, J. D., Martin, J. J., Kyle, W. E. & Harris, B. J. (1978). *Arch. Biochem. Biophys.* **191**, 153–160.
- Garrow, T. A. (1996). *J. Biol. Chem.* **271**, 22831–22838.
- Jancarik, J. & Kim, S.-H. (1991). *J. Appl. Cryst.* **24**, 409–411.
- Lee, K. H., Cava, M., Amiri, P., Ottoboni, T. & Lindquist, R. N. (1992). *Arch. Biochem. Biophys.* **292**, 77–86.
- McPherson, A. (1976). *J. Biol. Chem.* **251**, 6300–6303.
- Matthews, B. W. (1968). *J. Mol. Biol.* **33**, 491–497.
- Millian, N. S. & Garrow, T. A. (1998). *Arch. Biochem. Biophys.* **356**, 93–98.
- Mudd, S. H., Levy, H. L. & Skovby, F. (1995). *The Metabolic and Molecular Bases of Inherited Disease*, edited by C. R. Scriver, A. L. Beaudet, W. S. Sly & D. Vale, pp. 1279–1327. New York: McGraw-Hill.
- Otwinowski, Z. & Minor, W. (1997). *Methods Enzymol.* **276**, 307–326.
- Tong, L. & Rossmann, M. G. (1997). *Methods Enzymol.* **276**, 594–611.